PROCEEDINGS OF SCIENCE

Measurement of Neutron Recoil Polarization in Deuteron Photodisintegration

Thomas Krahulik,[a,*] **Blaine Norum,**[a] **Robert Pywell,**[b] **Tanner Polischuk,**[b] **Haoyu Chen,**[a] **Matthew Roberts**[a] **and Werner Tornow**[c]

[a] *University of Virginia, Charlottesville, VA, United States*
[b] *University of Saskatchewan, Saskatoon, Saskatchewan, Canada*
[c] *Duke University, Durham, NC, United States*

E-mail: ttt5kq@virginia.edu

An experiment at the High Intensity Gamma Source (HIGS) at the Triangle University Nuclear Laboratory (TUNL) was recently performed to measure the polarization of recoiling neutrons from photodisintegration of deuterium nuclei. As the simplest, multi-body nucleus, the deuteron offers a unique opportunity to study nucleon-nucleon interactions. Over the years, nuclear theory has developed to be able to describe the behavior and structure of few-body nuclei fairly well. However, discrepancies between theory and experimental data persist in measurements of polarization observables. The recoil polarization in $d(\gamma,\vec{n})p$ is a prime example of such a measurement. The purpose of the experiment is to map the polarization transfer for photon energies below 20 MeV and three laboratory angles. The setup consists of high pressure ^{4}He-Xe polarization analyzers surrounded by neutron scintillation counters to measure the asymmetry in the scattering of polarized neutrons. From this measurement, the polarized and unpolarized photon beam contributions to the neutron polarization will be extracted and compared to theory.

25th International Spin Symposium (Spin 2023)
24-29 September, 2023
Durham, NC, United States

*Speaker

PoS(SPIN2023)172

1. Introduction

Over the years, nuclear theory has developed various nuclear potentials to model nucleon-nucleon interactions in the low energy regime. These potentials provide a means for understanding the structure and reactions of light nuclei by building up the interactions between nucleons. Theoretical calculations of physical observables for nuclear bound states and nucleon scattering have been compared with experimental measurements to test their efficacy. Cross section calculations have demonstrated reasonable agreement with contemporary models, however discrepancies begin to appear when considering certain polarization observables.

As the only stable two-nucleon bound state, the deuteron is a prime testing ground for nuclear potentials models. Due to the well-understood behavior of the electromagnetic interaction, photodisintegration of the deuteron can offer experimentally accessible measurements to test models of the nucleon-nucleon interaction. One such measurement is the polarization of recoil neutrons from the photodisintegration process. Historical experimental data on this observable departs from theoretical predictions for photon energies below 20 MeV. Figure 1 shows collective data from Nath et al. [1] and Holt et al. [2] compared to calculations performed by H. Arenhövel [3, 4].

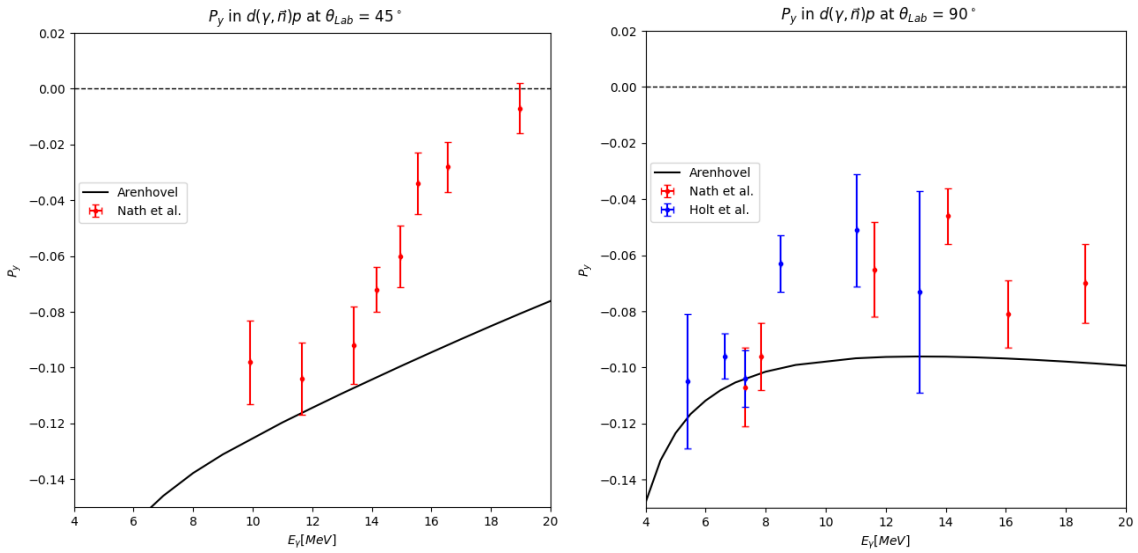

(a) Comparison of P_y experimental data with theoretical calculation at $\theta_{Lab} = 45°$

(b) Comparison of P_y experimental data with theoretical calculation at $\theta_{Lab} = 90°$

Figure 1: Historical experimental data of P_y in deuteron photodisintegration compared to theoretical calculations performed by H. Arenhövel

Since the measurements providing the data in Figure 1, accelerator technology has developed to provide better performance in beam energy resolution and control. With these developments in accelerator science, the purpose of this experiment is to revisit some of these measurements with modern capabilities as a robust test of the nuclear theory. The experiment intends to map the polarization of the recoil neutrons from $d(\gamma,\vec{n})p$ for energies below 20 MeV at lab angles of $\theta_{Lab} = 45°, 90°,$ and $135°$. The measurement will also allow for the extraction of contributions to the neutron polarization from both unpolarized and polarized photons.

2. Measurement

The basic measurement of the experiment is the asymmetry (Eq. 1) in the scattering of spin up (+) vs. spin down (-) neutrons.

$$A(\theta) = \frac{\sigma_+ - \sigma_-}{\sigma_+ + \sigma_-} \tag{1}$$

This asymmetry presents as a left-right asymmetry in the scattering angle, θ, of the neutrons, the magnitude of which depends on the polarization of the neutrons. The neutrons scatter from an analyzing material with well-defined analyzing power, A_y, allowing a calculation of the measured neutron polarization, P_y^m with Eq. 2.

$$A(\theta) = P_y^m A_y(\theta) \tag{2}$$

P_y^m is correlated with polarization contributions from both unpolarized photons (P_y^u) and polarized photons (P_y^l) as shown in Eq. 3 [3]. These quantities vary with the polar angle of photoneutrons, θ_n, which is mapped by this experiment for three different values of θ_n.

$$P_y^m \frac{d\sigma(P_y^\gamma, \theta_n, \phi_n)}{d\Omega} = \frac{d\sigma(\theta_n)}{d\Omega}\bigg|_{P_y^\gamma=0} \left[P_y^u(\theta_n) + P_y^\gamma P_y^l(\theta_n) \cos(2\phi_n) \right] \tag{3}$$

Each contribution can be determined by varying the polarization of the incident photon beam. A circularly polarized beam ($P_y^\gamma = 0$) can isolate P_y^u, and then a linearly polarized beam ($P_y^\gamma = 1$) can offer a means to calculate P_y^l once P_y^u is known.

3. Experimental Setup

3.1 High Intensity Gamma Source

The experiment was hosted at the High Intensity Gamma Source (HIGS or HIγS) at the Triangle Universities Nuclear Laboratory (TUNL). HIGS uses Compton backscattering of photons to produce monoenergetic gamma beams with an energy resolution of about 3%. For energies below 20 MeV, the accelerator can provide a flux on the order of 10^9 photons per second, making the facility the most intense source of gamma photons in the world. Additionally, HIGS can provide high polarization for these gamma-ray beams, achieving over 95% for either linear or circular polarization. [6] These capabilities provide ideal parameters for this experiment of $d(\gamma, \vec{n})p$ with high statistics for precise measurements.

3.2 Detector Arrangement

At the center of the setup is a cylindrical, heavy water (^2H_2O) target of length 20 cm and diameter 4 cm. Surrounding the target are six "stations" of detectors, two at each laboratory angle of 45°, 90°, and 135°. These stations allow measurements of neutron polarization for these three angles of photoneutrons, providing direct comparisons to the historical data in Figure 1. The 45° and 135° stations are at $\phi = 0°$ and $\phi = 180°$, while the 90° stations are at $\phi = 90°$ and $\phi = 270°$. This simplifies calculations of the polarization contributions in Eq. 3 since $\cos(2\phi_n) = \pm 1$. Each station

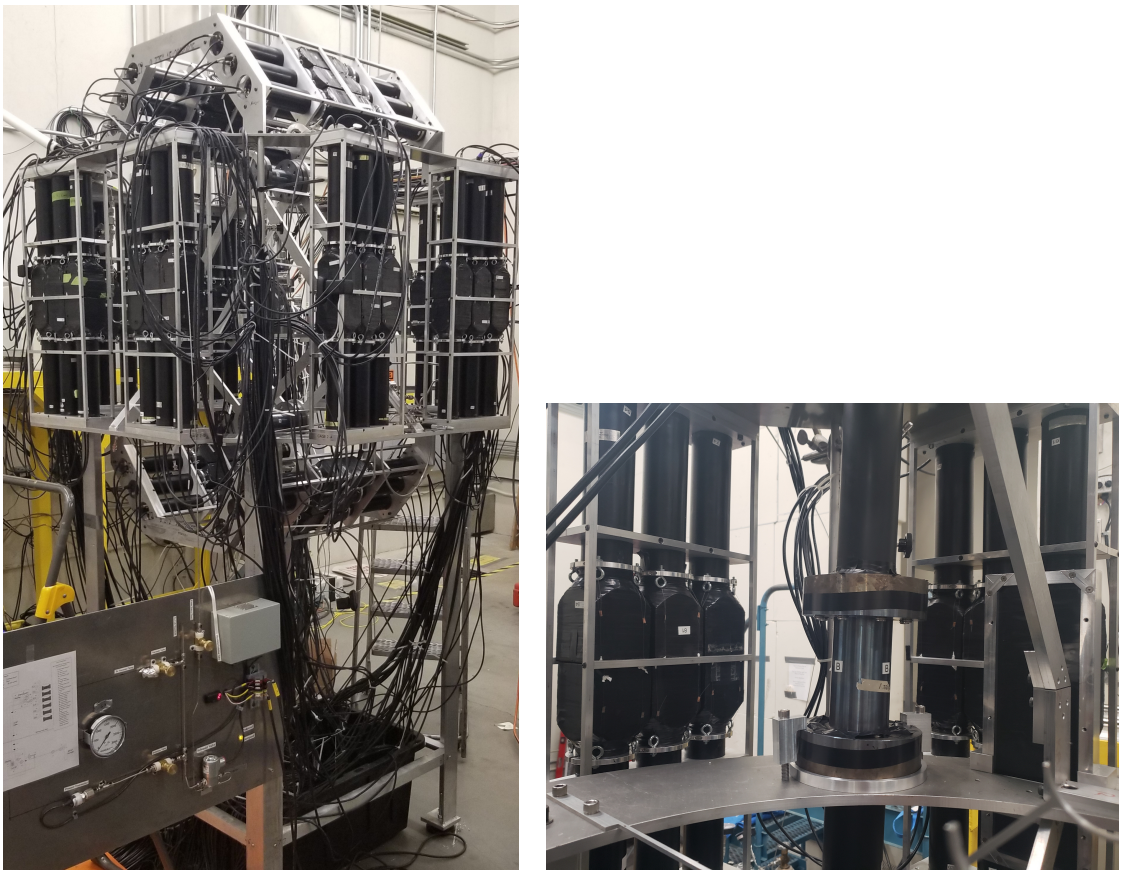

(a) Full view of experimental setup

(b) Close up view of detector station from target

Figure 2: Images showing structure and details of the experimental setup

consists of a polarization analyzer with two groups of neutron counting detectors on either side of the analyzer, enabling measurements of the left-right asymmetry in polarized neutron scattering. Figure 2 shows an image of the experimental setup alongside a closer look at the arrangement of a detector station.

The polarization analyzers for this experiment are high pressure ^{4}He-Xe gas scintillating detectors. This type of detector has proven to be effective for neutron detection [7, 8], with the helium acting as the analyzing material. Helium has well defined analyzing powers, A_y, for neutron energies below 20 MeV [9], allowing for calculations of neutron polarization with Eq. 2. Recoiling helium nuclei in the analyzers excite xenon atoms that in turn scintillate. The light output is detected by photomultiplier tubes (PMTs) on each end of the analyzer, providing a signal that indicates when a neutron has scattered in a polarization analyzer.

The analyzers contain a cylindrical active volume of 11.83 cm height and 6.00 cm diameter with 2.5 mm thick steel walls. They are operated at an internal gas pressure of 2500 PSI, with a 9:1 ratio for the ^{4}He-Xe mixture. At each end of the analyzer is a 1.9 cm thick glass window to enable light output to the PMTs. The inner walls of the cylinder are coated with a MgO layer about 1 mm thick to act as a reflector to reduce light loss. Diphenylstilbene (DPS) is deposited on the inside surfaces of the analyzer to wavelength shift the scintillation light from ultraviolet to visible

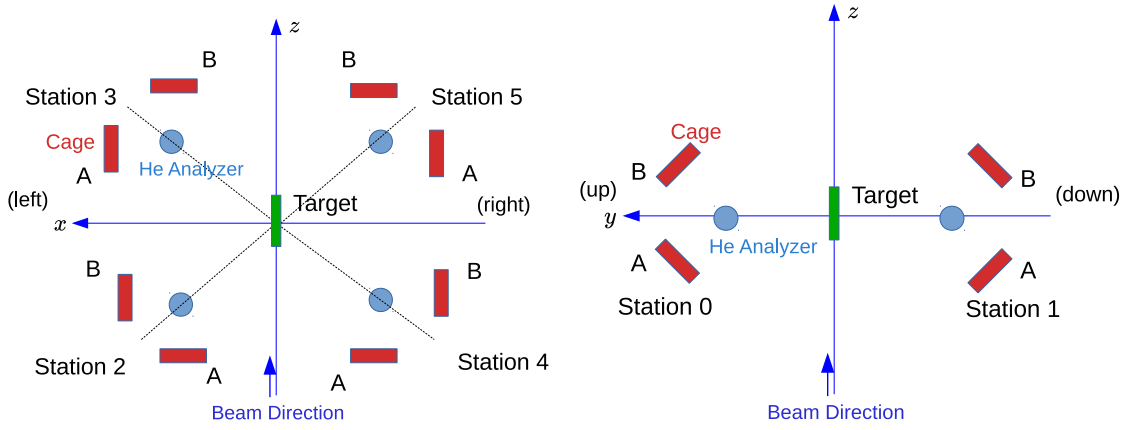

(a) In-plane layout **(b)** Out-of-plane layout

Figure 3: Schematic of experimental layout provided by T. Polischuk

light detected by the PMTs. This includes a layer of DPS on the inside of each window with a thickness of 50 $\frac{\mu g}{cm^3}$ and a layer on the inner walls of the analyzer (on top of the MgO reflector) with a thickness of 200 $\frac{\mu g}{cm^3}$.

On each side of an analyzer is a set of six scintillating neutron detectors for counting neutrons scattering left or right from the analyzers. These detectors are organic liquid scintillating (BC-505) detectors borrowed from the *Blowfish* detector array. [10] BC-505 is used for its capabilities in pulse-shape discrimination for identifying between neutrons and photons, while being a chemically safer alternative to other liquid scintillators. Each detector has an active volume of liquid scintillator of 7.6 cm X 7.6 cm X 6.4 cm contained in a Lucite cell. These cells are connected to PMTs through a light guide for detecting the scintillation light. [10]

4. Analysis

Data collection of the experiment has been completed and analysis is currently ongoing. The asymmetry is measured by the differences in neutron yields on the two sides of each analyzer. To calculate these yields, the analysis must determine which signals from PMTs correspond to the polarized neutrons of interest.

4.1 Pulse Shape Discrimination

As discussed in Section 3.2, the *Blowfish* detectors used for neutron counting are designed for efficient pulse shape discrimination (PSD) to differentiate between signals from neutrons and photons. Neutrons generate a delayed light output in the liquid scintillator as compared to photons, a characteristic that manifests as a broader waveform in the signal from the PMTs. The PSD is quantified with the calculation shown in Eq. 4.

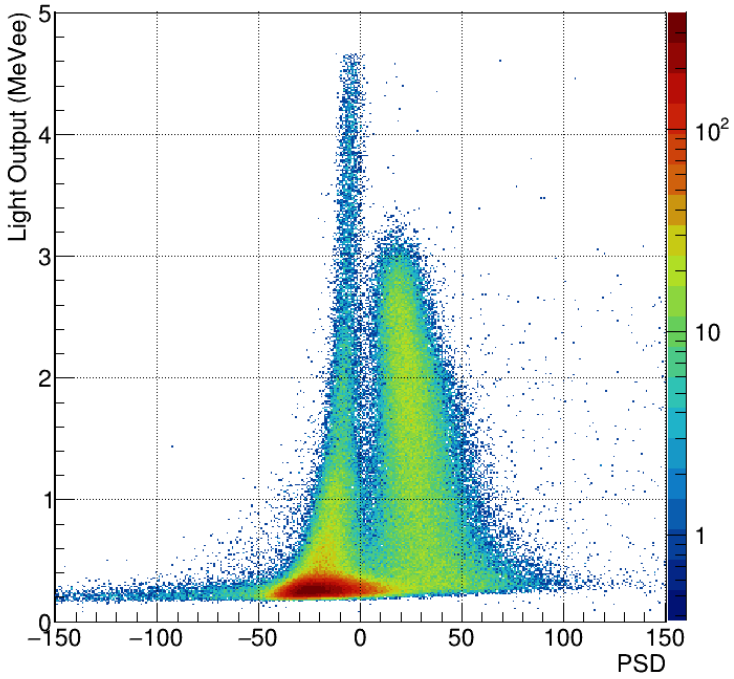

$$PSD = \frac{Q_{long} - Q_{short}}{Q_{long}} \quad (4)$$

Figure 4: Sample histogram of PSD plotted against Light Output, measured in MeV electron equivalent (MeVee). The two peaks demonstrate the separation of gammas (left) and neutrons (right) as a function of PSD.

The difference between long gate and short gate charge integration over the waveforms reveals a separation in signals of neutrons and photons. A PSD cut is then applied to the data to remove signals from gammas.

4.2 Timing Cuts

While the measurement relies on photoneutrons that scatter in an analyzer before detection in the neutron counters, some neutrons will have different trajectories through the experimental setup. They could travel directly from the target to the counters without first passing through the analyzer or they could scatter from another part of the setup, such as the experimental frame, before being detected. These neutrons also need to be filtered out of the data, since they provide no information about the asymmetry due to the polarization. This is accomplished with timing techniques in the analysis.

The first way to ensure measurement of neutrons of interest is to require coincident signals between an analyzer and a neutron counter. There should be a rapid sequence of signals received as a neutron passes through the setup, first from the analyzer PMTs, then from a neutron detector. Requiring both signals to be measured cuts out neutrons that will not provide accurate measurements of their polarization.

With the high intensity of the gamma beam, there is the chance of accidental coincidences between the detectors, as scattered gammas can also generate signals. For the beam energies in

this experiment, a photoneutron will be traveling much slower than the speed of light, resulting in a measurably longer time of flight than gammas. Using a timing trigger provided by the accelerator, an expected time of flight (within a small uncertainty) can be calculated for a neutron and used to cut out signals that were measured too soon, indicating detection of photons.

4.3 Geometric Asymmetries

The analysis must also account for asymmetries in neutron yields due to the finite length of the target. Attenuation of the gamma-ray beam through the target results in lower production of photoneutrons towards the downstream end of the target. Based on the geometry of the setup, this will generate an asymmetry in the trajectories of neutrons as they travel to the analyzers, and then scatter to either side. Within each station, the downstream detectors will measure higher count rates because of this, requiring a correction to the measured asymmetry. The correction factor is calculated with a full simulation of the experimental setup in Geant4 [11–14]. Since Geant4 does not account for the asymmetries in scattering due to the polarization of the neutrons, asymmetries calculated by analyzing simulation data provide the geometric asymmetries. Simulations for each beam energy have been performed, and correction factors to the asymmetry have been incorporated into analysis of the experimental data.

5. Summary

An experiment measuring the neutron polarization in $d(\gamma, \vec{n})p$ has been performed for photon energies below 20 MeV, taking advantage of the capabilities of HIGS at TUNL to produce intense, monoenergetic, polarized gamma-ray beams. Data was collected at photon energies of $E_\gamma = 8, 12,$ and 16 MeV, to investigate prior discrepancies between experimental measurements and theoretical calculations (Fig. 1). The measurement maps the neutron polarization at laboratory angles of $\theta_{Lab} = 45°, 90°,$ and $135°$. From the measured polarization, the unpolarized and polarized photon beam contributions can be extracted. Analysis of the data is in progress.

Acknowledgements

This experiment owes much of its successful operation to the diligence and dedication of the TUNL faculty and staff. This work supported in part by the U.S. Department of Energy under grant No. DE-SC0016443. The authors also acknowledge the financial support of the Natural Sciences and Engineering Research Council of Canada. This research was enabled in part by support from the Digital Research Alliance of Canada (https://alliancecan.ca) including the partners, the BC DRI group and the Prairies DRI.

References

[1] R. Nath, F. W. K. Firk, and H. L. Schultz. "Differential Polarization of Photoneutrons from Deuterium". *Nuclear Physics A* **194**, 49-63 (1972).

[2] R. Holt, *et al.* "Meson Exchange Currents and the Reaction $^2H(\gamma, n_{pol})H$". *Phys. Rev. Lett.* **50**, no. 8, 577-579 (1983).

[3] H. Arenhövel and M. Sanzone. "Photodisintegration of the Deuteron: A Review of Theory and Experiment". *Few Body Systems* Suppl. **3** (1991).

[4] H. Arenhövel. Private Communication.

[5] B.E. Norum, *et al.* "Measurement of Neutron Recoil Polarization in Low Energy Photodisintegration of Deuterium". [Proposal to the High Intensity Gamma-ray Source PAC-12]. Internal Document. (2013).

[6] Y. K. Wu, *et al.* "Performance and Capabilities of Upgraded High Intensity Gamma Source at Duke University". *Proc. of the 23rd Particle Accelerator Conference* 3181-3183 (2009).

[7] J. A. Northrop and J. C. Gursky. "Relative Scintillation Efficiencies of Noble Gas Mixtures". *Nucl. Instr.* **3**, no. 4, 207-212 (1958).

[8] W. S. Wilburn, C. R. Gould, G. M. Hale, P. R. Huffman, C. D. Keith, N. R. Roberson, and W. Tornow. "Measurements at Low Energies of the Polarization Transfer Coefficient $K_y^{y'}$ for the Reaction $^3H(\vec{p}, \vec{n})^3He$ at 0°". *Few Body Systems* **24**, 26-38 (1998).

[9] T. Stammbach and R. L. Walter. "R-Matrix Formulation and Phase Shifts for n-^{4}He and p-^{4}He Scattering for Energies Up to 20 MeV". *Nucl. Phys. A* **180**, 225 (1972).

[10] B. Sawatzky. Ph.D. Thesis, University of Virginia (2005).

[11] Geant4 Collaboration. Geant4 User's Guide for Application Developers. (2011).

[12] J. Allison *et al.* "Recent Developments in Geant4". *Nucl. Instrum. Meth. A*. **835**, 186-225 (2016).

[13] J. Allison *et al.* "Geant4 Developments and Applications". *IEEE Trans. Nucl. Sci.*. **53**, 270-278 (2006).

[14] S. Agostinelli *et al.* "Geant4 - A Simulation Toolkit". *Nucl. Instrum. Meth. A*. **506**, 250-303 (2003).